Research Square

Preprints are preliminary reports that have not undergone peer review.
They should not be considered conclusive, used to inform clinical practice,
or referenced by the media as validated information.

Jost function for the description of resonance in finite quantum multichannel systems

Kazuhito Mizuyama

mizukazu147@gmail.com

Research Article

Keywords: Jost function, Resonance, Hartree-Fock-Bogoliubov, Random-phase approximation, Fano effect

Posted Date: January 13th, 2026

DOI: https://doi.org/10.21203/rs.3.rs-8501414/v1

License: This work is licensed under a Creative Commons Attribution 4.0 International License.
Read Full License

Additional Declarations: No competing interests reported.

Version of Record: A version of this preprint was published at Few-Body Systems on March 10th, 2026.
See the published version at https://doi.org/10.1007/s00601-026-02032-z.

Jost function for the description of resonance in finite quantum multichannel systems

Kazuhito Mizuyama

Received: date / Accepted: date

Abstract The Jost function is defined as the coefficient function connecting the regular and irregular solutions of the fundamental differential equations. It is known that the zeros of the Jost function on the complex energy plane correspond to the poles of the S-matrix, which represent the complex eigenvalues of bound and resonant states. This paper reviews our recent extensions of the Jost function method to nuclear multichannel systems, specifically within the frameworks of the Hartree-Fock-Bogoliubov (HFB) theory and the Random Phase Approximation (RPA) theory (Jost-RPA method). A unitary S-matrix is derived using these extended Jost functions. By focusing on the poles of the S-matrix, we attempt to analyze and classify the resonances. We discuss three key applications: (1) the extraction of Fano parameters to analyze asymmetric line shapes in neutron scattering within the HFB framework, (2) the decomposition of the RPA strength function using eigenphase shifts, and (3) the application of the Mittag-Leffler theorem to decompose the RPA response into contributions from individual resonance poles.

Keywords Jost function · Resonance · Hartree-Fock-Bogoliubov · Random-phase approximation · Fano effect

1 Introduction

In nuclear physics, there are mainly two phenomena referred to as "resonance." One appears in nuclear reactions, and the other refers to a collective excitation of the nuclear structure (e.g., the giant resonance). Classically, "resonance" refers to a vibration phenomenon. In quantum scattering theory, a resonance as a metastable state appears as a peak with a finite width in the cross section.

Theoretically, resonances are often classified based on their formation mechanism. One is the *shape resonance*, which occurs due to the trapping of a particle

K. Mizuyama
Institute of Research and Development, Duy Tan University, Da Nang 550000, Vietnam
Faculty of Natural Sciences, Duy Tan University, Da Nang 550000, Vietnam
E-mail: mizukazu147@gmail.com

by a potential barrier, such as the centrifugal barrier. The other is the *Feshbach resonance* [1], which arises from the coupling between an open channel (continuum state) and a closed channel (bound state). In nuclear physics, collective excitations like giant resonances often involve complex interplays of these mechanisms. Despite their different physical origins, both types of resonances are mathematically unified as poles of the S-matrix on the complex energy plane.

Specifically, in systems where a discrete state is coupled to a continuum background, such as in Feshbach resonances, quantum interference occurs between the direct transition to the continuum and the transition via the resonant state. This interference leads to a characteristic asymmetric line shape in the cross section, known as the Fano profile [2]. Consequently, the simple Breit-Wigner formula may not be sufficient to describe the resonance structure accurately. Therefore, a unified theoretical framework capable of locating the S-matrix poles directly on the complex energy plane is essential for a comprehensive understanding of nuclear resonances.

The Jost function was originally formulated for single-channel systems [3]. However, it can also be defined for multi-channel systems, since the Jost function is given as a coefficient function which connects the regular and irregular solutions. In our recent works, we extended the Jost function within the framework of the Hartree-Fock-Bogoliubov (HFB) theory [4] and the Random Phase Approximation (RPA) theory [5].

In this paper, we present an overview of these extended Jost function methods. In Sec. 2, we introduce the HFB Jost function and the RPA Jost function. In Sec. 3, we show how to analyze resonances using the Fano effect, the eigenphase shift decomposition, and the Mittag-Leffler theorem. Finally, Sec. 4 is devoted to the summary and future perspectives.

2 Extension of the Jost Function to Multichannel Systems

The definition of the Jost function in single-channel scattering theory is extended to multichannel systems. In both the Jost-HFB and Jost-RPA frameworks, the fundamental equations are given as a system of coupled differential equations in coordinate space. In this section, we explain how to construct the Jost function matrix in these theories to deal with the continuum boundary conditions and find the S-matrix poles. We first discuss the HFB case for quasiparticle resonances, and then the RPA case for collective excitations.

2.1 HFB Jost function

To describe quasiparticle resonances including pairing correlations, we extended the Jost function to the HFB formalism in Ref. [4]. The HFB equations are given as a set of coupled differential equations for the particle and hole components of the quasiparticle wave function in coordinate space.

For a spherical system, the radial HFB equation for a quasiparticle with energy E takes the matrix form:

$$\left[\frac{d^2}{dr^2} + \mathcal{K}^2(E) - \frac{2m}{\hbar^2}\sigma_z \mathcal{U}_{lj}(r)\right] \phi_{lj}(r, E) = 0, \tag{1}$$

where ϕ_{lj} represents the two-component spinor consisting of the upper (particle) and lower (hole) radial wave functions. The potential term $\mathcal{U}_{lj}(r)$ includes the mean-field potential and the centrifugal potential $U_{lj}(r)$, and the pairing field $\Delta(r)$ which couples the particle and hole channels, defined as:

$$\mathcal{U}_{lj}(r) = \begin{pmatrix} U_{lj}(r) & \Delta(r) \\ \Delta(r) & -U_{lj}(r) \end{pmatrix}. \tag{2}$$

The momentum matrix $\mathcal{K}(E)$ is defined by

$$\mathcal{K}(E) = \begin{pmatrix} k_1(E) & 0 \\ 0 & k_2(E) \end{pmatrix} \tag{3}$$

with $k_1(E) = \sqrt{\frac{2m}{\hbar^2}(\lambda + E)}$ and $k_2(E) = \sqrt{\frac{2m}{\hbar^2}(\lambda - E)}$, where λ is the chemical potential. The HFB equation, given by the 2×2 simultaneous second-order differential equations, contains four linearly independent solutions in total: two regular solutions ($\phi_{lj}^{(r1)}$ and $\phi_{lj}^{(r2)}$) and two irregular solutions ($\phi_{lj}^{(\pm 1)}$ and $\phi_{lj}^{(\pm 2)}$), due to the existence of different boundary conditions for each.

By defining the 2×2 regular solution matrix $\Phi_{lj}^{(r)}$ and the irregular solution matrix $\Phi_{lj}^{(\pm)}$ as

$$\Phi_{lj}^{(r)} = \begin{pmatrix} \phi_{lj}^{(r1)} & \phi_{lj}^{(r2)} \end{pmatrix} \text{ and } \Phi_{lj}^{(\pm)} = \begin{pmatrix} \phi_{lj}^{(\pm 1)} & \phi_{lj}^{(\pm 2)} \end{pmatrix} \tag{4}$$

the Jost function matrix $\mathcal{J}_{lj}^{(\pm)}$ is defined as the coefficient function matrix which connects the regular and irregular solution matrices as

$$\Phi_{lj}^{(r)\mathsf{T}} = \frac{1}{2}\left[\mathcal{J}_{lj}^{(+)}\Phi_{lj}^{(-)\mathsf{T}} + \mathcal{J}_{lj}^{(-)}\Phi_{lj}^{(+)\mathsf{T}}\right]. \tag{5}$$

Since the wavenumbers $k_1(E)$ and $k_2(E)$ are double-valued functions, the first Riemann sheet is defined as the energy which satisfies Im $k_1(E) > 0$ and Im $k_2(E) > 0$. It is analytically connected to the second Riemann sheet, defined as the energy which satisfies Im $k_1(E) < 0$ and Im $k_2(E) > 0$, on the real axis where $E > -\lambda$. The third Riemann sheet, defined as the energy satisfying Im $k_1(E) > 0$ and Im $k_2(E) < 0$, is analytically connected to the first Riemann sheet on the real axis where $E < \lambda$. The S-matrix poles E_n are given as solutions satisfying

$$\det[\mathcal{J}_{lj}^{(+)}(E_n)] = 0. \tag{6}$$

There are bound solutions on the first Riemann sheet and resonance poles on the second Riemann sheet. The poles found on the third Riemann sheet are negative-energy solutions of the resonance poles found on the second Riemann sheet. This approach allows us to find the complex eigenvalues of the HFB Hamiltonian without relying on boundary condition discretization.

In Fig. 1, we show the trajectories of the S-matrix poles for the neutron $d_{5/2}$ state as a function of the average pairing gap $\langle\Delta\rangle$. The poles are determined by the zeros of the Jost function determinant. As the pairing gap increases, the poles move on the complex energy plane, indicating the change in the resonance properties due to the pairing correlation. The trajectories clearly demonstrate how the bound states and resonant states evolve and interact under the influence of the pairing field.

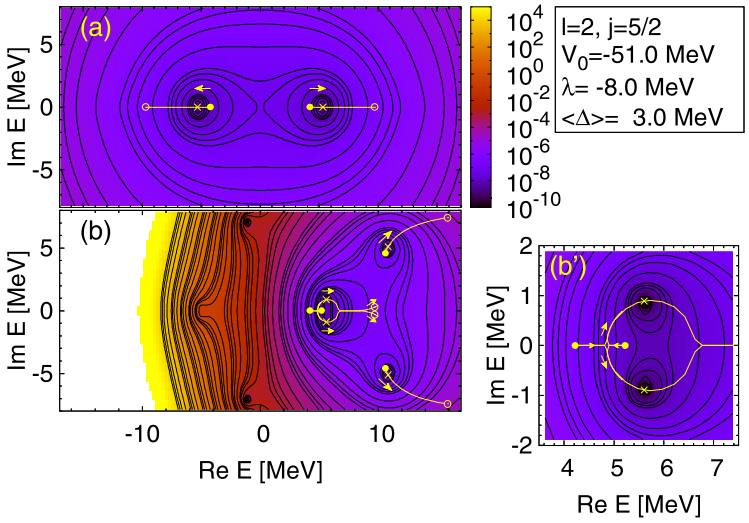


Fig. 1 The absolute square of the $\det[\mathcal{J}^{(+)}_{lj}(E)]$ for $d_{5/2}$ with $\langle\Delta\rangle = 3.0$ MeV and $\lambda = -8.0$ MeV shown on (a) the first Riemann sheet and (b) second Riemann sheet of the complex quasiparticle energy plane. The yellow X symbols show the position of zeros which represent the poles of the S-matrix. The yellow curves are the trajectories of zeros obtained by varying the pairing gap $\langle\Delta\rangle$ from 0.0 (solid circle) to 10.0 (open circle) MeV. The arrows represent the direction of X. Adapted from Ref. [4].

2.2 RPA Jost function

Giant resonances and other collective excitation modes in nuclei are attributed to residual interactions within the RPA theory. As shown in Ref. [5], the RPA equations in coordinate space can be formulated as a system of simultaneous differential equations involving a $2N \times 2N$ matrix, where N denotes the number of particle-hole configuration channels.

In the Jost-RPA method, the fundamental equation for the RPA state with excitation energy $\hbar\omega$ is given as a coupled differential equation:

$$\left[\frac{d^2}{dr^2} + \mathcal{K}^2(\omega) - \frac{2m}{\hbar^2}\mathcal{V}_{RPA}(r)\right]\phi(r,\omega) = 0, \tag{7}$$

where $\phi(r,\omega)$ is a $2N$-component vector containing the forward (X) and backward (Y) amplitudes for all configuration channels which can be expressed as

$$\phi^{\mathsf{T}} = \left(X_1 \cdots X_N\ Y_1 \cdots Y_N\right) \tag{8}$$

$\mathcal{K}(\omega)$ is a $2N\times 2N$ diagonal matrix which is expressed by the momentum component $k_{1,i}(\omega)(=\sqrt{\frac{2m}{\hbar^2}(\epsilon_i+\omega)})$ for the forward amplitude and $k_{2,i}(\omega)(=\sqrt{\frac{2m}{\hbar^2}(\epsilon_i-\omega)})$, where ϵ_i is the hole state energy. The potential $2N\times 2N$ matrix $\mathcal{V}_{RPA}$ includes the unperturbed mean-field potentials and the residual interaction which couples different particle-hole channels. The $2N \times 2N$ simultaneous second-order differential equation has $2N$ types of solutions, obtained with different boundary conditions for regular and irregular solutions respectively. Using these $2N$ types of solutions,

the $2N \times 2N$-dimensional regular solution and irregular solution matrices ($\Phi^{(r)}$ and $\Phi^{(\pm)}$) are defined as,

$$\Phi^{(r)} = \left(\phi^{(r1)} \cdots \phi^{(r-2N)}\right) \text{ and } \Phi^{(\pm)} = \left(\phi^{(\pm 1)} \cdots \phi^{(\pm 2N)}\right) \tag{9}$$

and the Jost function is defined as a coefficient matrix function which connects the regular solution and irregular solution matrices as,

$$\Phi^{(r)\mathsf{T}} = \frac{1}{2}[\mathcal{J}^{(+)}\Phi^{(-)\mathsf{T}} + \mathcal{J}^{(-)}\Phi^{(+)\mathsf{T}}]. \tag{10}$$

The poles associated with RPA excited states are determined by solving the condition:

$$\det[\mathcal{J}(\omega)] = 0 \tag{11}$$

on the complex energy plane ω. These poles lie on various Riemann sheets connected by branch cuts opening at different threshold energies. It is important to identify the correct Riemann sheet for determining the physical excitation energy and decay width. For example, in the E1 excitation of ^{16}O, only a few sheets are physically relevant for the observable giant resonance.

Figure 2 displays the E1 strength function of ^{16}O and the corresponding poles on different Riemann sheets. The peaks in the strength function are associated with specific poles, labeled (a)–(g). The analysis of the Jost function determinant $|\det \mathcal{J}|$ on the complex energy sheets allows us to identify which poles contribute to the physical strength function observed on the real axis.

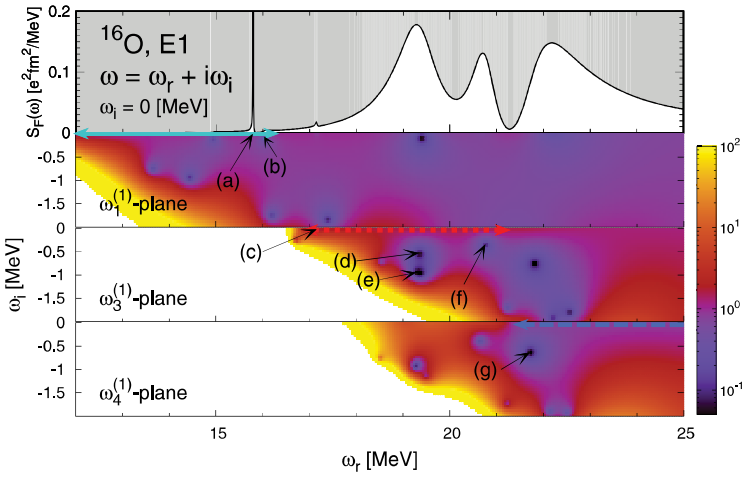


Fig. 2 The E1 strength function of ^{16}O plotted as a function of ω_r with $\omega_i = 0$ MeV in the upper panel, and $|\det \mathcal{J}(\omega_i^{(1)})|/|\det \mathcal{J}(\omega_0)|$ for $i \in 1, 3$, and 4 in the lower three panels. The poles labeled (a)–(g) are poles which can contribute to the strength function. The sky-blue solid, red dotted, and blue dashed lines (with both side arrows) denote the branch cut lines for three Riemann sheets ($\omega_1^{(1)}$,$\omega_3^{(1)}$ and $\omega_4^{(1)}$ which connect with the first Riemann sheet (ω_0). Adapted from Ref. [5].

3 Analysis of Resonance

Based on the Jost function formalism extended to the HFB and RPA theories described in the previous section, we have performed systematic analyses of resonances in various nuclear systems. The primary advantage of our method is the ability to directly determine the S-matrix poles on the complex energy plane, which allows for a clear classification of resonances even in cases where the background continuum is significant. In this section, we present three key applications of our developed methods: the analysis of the Fano effect in nucleon-nucleus scattering, the decomposition of RPA strength functions, and the Mittag-Leffler expansion of the response function. These studies clarify the detailed properties of resonances from the viewpoint of the S-matrix poles.

3.1 Fano effect

The Fano effect describes the interference between a discrete state and a continuum background, which is known in atomic physics [2]. In Ref. [6], we showed that in nucleon-nucleus scattering, even when S-matrix and K-matrix poles exist simultaneously, the scattering wave function may not have a typical resonant feature due to the Fano effect.

Using the Jost-HFB formalism, we derived the Fano parameters. It is found that pairing correlations affect the Fano asymmetry parameter q. In stable nuclei, neutron elastic scattering cross sections often show strong asymmetry. On the other hand, in unstable nuclei, the line shapes tend to be symmetric Breit-Wigner forms.

Figure 3 shows the numerical results for the square of the T-matrix, the phase shift, and the extracted Fano parameters q and ϵ for the $p_{1/2}$ neutron scattering. The energy dependence of these quantities clearly illustrates the asymmetric resonance shape resulting from the interference with the continuum background.

3.2 Eigenphase-shift decomposition

In Ref. [7], we defined the S-matrix which satisfies unitarity in the Jost-RPA method. This unitarity allows us to decompose the RPA strength function using the eigenphase shifts obtained by diagonalization of the S-matrix.

The S-matrix is diagonalized by unitary matrices, and its eigenvalues are expressed by eigenphase shifts. This decomposition is useful to analyze physical quantities, such as the RPA strength function, transition densities, and wave functions, by decomposing them into contributions from states defined by these phases.

We applied this method to quadrupole excitations in ^{16}O. It is confirmed that the Coulomb interaction affects the mixing of isoscalar (IS) and isovector (IV) modes. The eigenphase shift decomposition clearly showed how the strength is redistributed due to this mixing.

Figure 4 presents the eigenphase shifts $\delta_\alpha^{(1)}$ and the decomposition of the RPA strength function. The positions of the S-matrix poles (complex energy) and K-matrix poles (real energy where phase shift crosses $\pi/2$) are also indicated. This

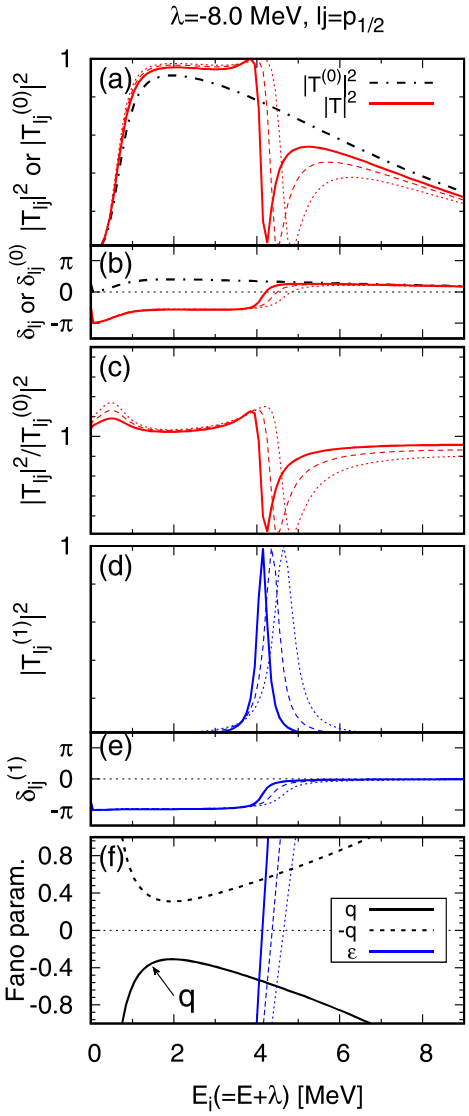


Fig. 3 The numerical results of square of T-matrix of the neutron elastic scattering, corresponding phase shift, and the Fano parameters q and ϵ for $p_{1/2}$ plotted as a function of the incident neutron energy $E_i(= E + \lambda)$ with $\lambda = -8.0$ MeV. Adapted from Ref. [6].

analysis clarifies the individual contributions of different eigenchannels to the total strength distribution.

3.3 Mittag-Leffler theorem

The Mittag-Leffler theorem [8–10] gives a representation for meromorphic functions in terms of their poles. In Ref. [11], we applied this theorem to the RPA

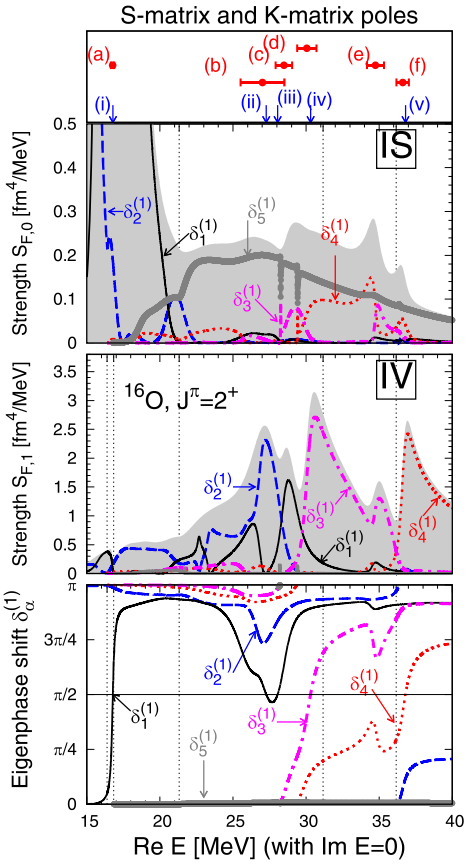


Fig. 4 Eigenphase shift $\delta_\alpha^{(1)}$ obtained by diagonalizing the S-matrix and decomposition of the RPA strength function by the eigenphase shift components (second and third panels). [(a)–(f)] in the upper figure are the S-matrix poles. The imaginary part of the poles is represented by error bars. [(i)–(v)] show the positions of the K-matrix poles appearing on the real axis of energy. The energy of the K-matrixpole is equivalent to the energy when the eigenphase shift $\delta_\alpha^{(1)}$ crosses $\pi/2$. Adapted from Ref. [7].

response function within the Jost-RPA framework. The response function $S_F(\omega)$ can be decomposed into a sum of pole terms and a background term:

$$S_F(\omega) = S_{F,\mathrm{bg}}(\omega) + \sum_g S^{(g)}_{F,\mathrm{pole}}(\omega). \tag{12}$$

Here, the pole term $S^{(g)}_{\mathrm{pole}}(\omega)$ is derived from the residue of the response function at the pole. In our approach, this residue is calculated via numerical contour integration enclosing the pole on the complex energy plane. This formulation enables us to analyze how much each resonance pole contributes to the total strength function.

We analyzed E1 giant resonances and quadrupole resonances in ^{16}O using this method. It is shown that while some peaks are dominated by a single pole, others result from the superposition of multiple poles. Also, we observed asymmetric peak

structures, which suggest the existence of Fano-type interference effects in nuclear excitations.

In Fig. 5, we demonstrate the decomposition of the RPA strength function into individual resonance pole contributions. The comparison between the total strength and the sum of pole terms highlights the role of the background term and the interference between overlapping resonances.

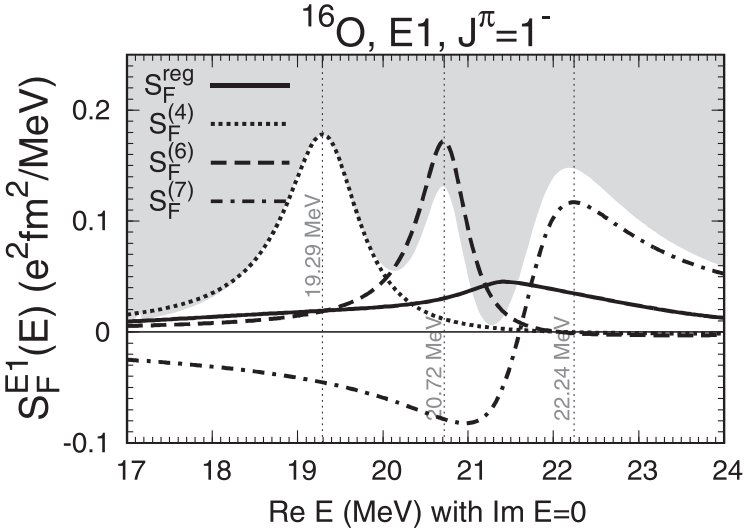


Fig. 5 Mittag-Leffler decomposition of the RPA strength function for ^{16}O into individual resonance pole contributions. Adapted from Ref. [11].

4 Summary and Future Perspectives

In this paper, we reviewed our recent advancements in extending the Jost function method to complex nuclear multichannel systems, specifically incorporating the frameworks of the Hartree-Fock-Bogoliubov (HFB) theory and the Random Phase Approximation (RPA). The core achievement of this work is the establishment of a robust framework that defines resonances strictly as poles of the S-matrix on the complex energy plane. By deriving a unitary S-matrix directly from the extended Jost function, we overcome the ambiguities associated with conventional discretization methods when dealing with continuum states. This approach allows for a unified and consistent description of bound, resonant, and continuum states.

We demonstrated the power and versatility of our method through three specific applications. First, the analysis of the Fano effect in neutron scattering revealed the crucial role of pairing correlations in determining the line shape of resonances. Second, the eigenphase-shift decomposition of RPA strength functions provided a clear physical picture of how different modes mix and contribute to the total strength. Third, the application of the Mittag-Leffler theorem enabled a quantitative decomposition of the RPA response into individual resonance pole

contributions, clarifying the structure of giant resonances and the role of the non-resonant background. These results underscore that the Jost function method is not merely a mathematical tool but a powerful physical approach to unveil the detailed properties of nuclear excitations.

Looking ahead, several promising directions for future research are envisioned. A primary objective is the application of the Jost-RPA method to heavier and more complex nuclei, including exotic nuclei near the drip lines. Such studies will be essential for understanding the nucleosynthesis and the structure of unstable nuclei where continuum coupling plays a dominant role. Another significant task is the extension of the formalism to describe nucleon-nucleus scattering on odd-mass targets, which requires a more complex treatment of angular momentum coupling. Furthermore, we are currently working on a proper orthonormalization of resonant states. This development will provide a complete basis set including resonances, enabling more advanced perturbative calculations and reaction theories. The extension of this framework to general finite quantum many-body systems beyond nuclear physics is also an exciting prospect, potentially offering new insights into resonance phenomena in various fields.

References

1. Feshbach, H.: Unified theory of nuclear reactions. Ann. Phys. (N.Y.) **5**, 357 (1958)
2. Fano, U.: Effects of Configuration Interaction on Intensities and Phase Shifts. Phys. Rev. **124**, 1866 (1961)
3. Jost, R., Pais, A.: On the scattering of a particle by a static potential. Phys. Rev. **82**, 840 (1951)
4. Mizuyama, K., Le, N. N., Thuy, T. D., Hao, T. V. N.: Jost function formalism based on the Hartree-Fock-Bogoliubov formalism. Phys. Rev. C **99**, 054607 (2019)
5. Mizuyama, K., Le, N. N., Thuy, T. D., Tung, N. H., Tam, D. Q., Hao, T. V. N.: Complex eigenenergy of the giant dipole resonance for ^{16}O by the Jost function within the random-phase approximation framework. Phys. Rev. C **107**, 024303 (2023)
6. Mizuyama, K., Le, N. N., Hao, T. V. N.: Fano effect on neutron elastic scattering by open-shell nuclei. Phys. Rev. C **101**, 034601 (2020)
7. Mizuyama, K., Thuy, T. D., Hao, T. V. N.: Eigenphase shift decomposition of the random-phase approximation strength function based on the Jost-RPA method. Phys. Rev. C **109**, 054304 (2024)
8. Rakityansky, S. A.: Jost Functions in Quantum Mechanics. Springer, Switzerland (2022)
9. Jeffreys, H., Jeffreys, B. S.: Methods of Mathematical Physics, 3rd ed. Cambridge University Press, Cambridge (1988)
10. Turner, L. E.: Historia Mathematica **40**, 36 (2013)
11. Mizuyama, K., Thuy, T. D.: Analysis of the contribution of resonance poles of ^{16}O based on the Mittag-Leffler theorem within the Jost random-phase approximation framework. Phys. Rev. C **111**, 054323 (2025)